The generalized-α method in mechatronic applications

Olivier Brüls* and Jean-Claude Golinval*

*LTAS-Vibrations et Identification des Structures, University of Liège,
Chemin des Chevreuils, 1, B52, B-4000 Liège

Abstract

This paper presents an extension of the generalized-α time-integrator to mechatronic systems represented by coupled first and second-order DAEs. A simple reformulation of those equations as full second-order DAEs allows the implementation of a monolithic integration scheme, so that the numerical dissipation properties are preserved, and second-order accuracy is obtained at least in the unconstrained case. The algorithmic parameters can be optimized either for the mechanical or the control subsystem. Two illustrative applications are treated in the fields of vehicle dynamics and robotics.

Key-words: Generalized-α method, multidisciplinary simulation, mechatronics, finite element method, block diagram language.

1 Introduction

For several years, the modelling and simulation of flexible multibody systems has reached a certain level of maturity. In particular, the finite element approach presented by Géradin and Cardona [1] allows a consistent description of large amplitude motions and deformations. The equations of motion are formulated as second-order differential-algebraic equations (DAEs) with index-3. Compared with approaches based on modal elastic coordinates, the finite element method allows a very systematic modelling process, it is more appropriate to deal with large nonlinear deformations, and the representation of the inertia forces is greatly simplified. However, due to the finite element discretization, a relatively high number of degrees-of-freedom is necessary to capture the dominant flexible modes of the physical system. Usually, accurate simulation results are only expected for the low-frequency modes of the model, whereas the contribution of the higher-order modes, which are typically poorly resolved, should be filtered by the numerical integration algorithm. For second-order ordinary differential equations (ODEs) in structural dynamics, the generalized-α method, which results from the successive contributions of Newmark [2], Hilber et al [3], and Chung and Hulbert [4], combines the advantages of one-step implementation, second-order accuracy, unconditional stability (A-stability) and adjustable high-frequency numerical damping. Erlicher et al [5] have studied its properties in the nonlinear regime, and Géradin and Cardona [1, 6] have shown that the damped generalized-α scheme can be efficiently applied in flexible multibody dynamics.

In a mechatronic system, the motion of the mechanism is driven by a control system composed of actuators, sensors, and control units. Therefore, a multidisciplinary simulation framework is required, where the dynamics of both the mechanism and the control system are considered. In previous contributions [7, 8], a unified environment has been proposed, where the mechanical system is modeled using the finite element approach [1], whereas the control system is described using the block diagram language. The strongly coupled equations of motion are thus formulated with a high level of modularity, and it is possible to implement a monolithic integration algorithm, as illustrated in Fig. 1. Since the control system is represented by first-order DAEs, the time-integration algorithm has to deal with mixed first and second-order DAEs.

A usual simulation method for mechatronic systems is to reformulate the second-order DAEs of the mechanism as first-order DAEs, and to apply any DAE integration scheme, such as Backward Difference Formulae (BDF) [9, 10, 11] or Implicit Runge-Kutta (IRK) methods [12]. Those methods can also be combined with an index reduction based on a constraint elimination technique or a constraint differentiation technique. However, for large scale structural models with broad frequency content and low physical damping, BDF and IRK schemes have some limitations. First,

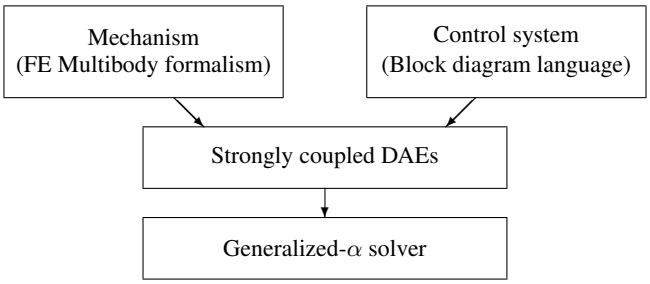

Figure 1: Strongly coupled and modular simulation strategy.

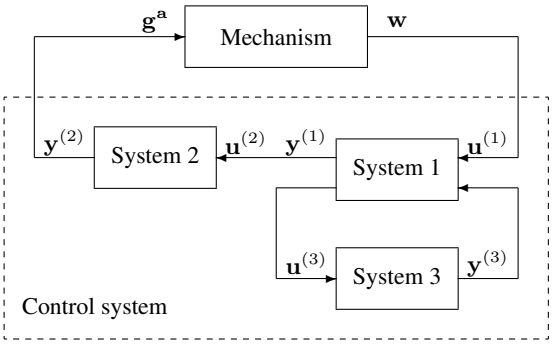

Figure 2: Model of a mechatronic system.

according to the second Dahlquist's barrier for multistep methods, unconditional stability is only possible if the order is lower or equal to 2, i.e. only BDF1 and BDF2 should be considered. Second, due to the coupling between the internal stages, fully implicit RK methods cannot be implemented with an efficiency comparable to the generalized-α method. Therefore, the attention is restricted to singly diagonally IRK methods, as discussed by Owren and Simonsen [13] for structural dynamic models.

The present paper demonstrates that the generalized-α method is an efficient tool for the simulation of flexible mechatronic systems. This work should be compared with the contribution of Negrut et al [14], who combined the HHT method for the mechanical variables with a one-step integration formula for the control state variables. Following this methodology, it is not possible to combine second-order accuracy with numerical damping for the state variables, even in the ODE case. Alternatively, a reformulation of the coupled equations as full second-order DAEs is proposed here, so that a monolithic generalized-α integrator can be used, and numerical dissipation can be introduced without destroying the order of accuracy, at least in the ODE case. After the description of the equations of motion (section 2) and of the time-integration algorithm (section 3), two realistic applications are presented in section 4: a vehicle semi-active suspension and a flexible manipulator with active vibration control.

2 Formulation of the equations of motion

Géradin and Cardona [1] have selected the finite element coordinates for the description of flexible multibody systems: each body is characterized by a set of nodes, and each node has its own translation and rotation coordinates. For spatial mechanisms, the absolute rotations are parameterized using the Cartesian rotation vector. The finite element coordinates are gathered in a $n \times 1$ vector $\mathbf{q}$ and they satisfy m kinematic constraints:

$$\mathbf{\Phi}(\mathbf{q}, t) = \mathbf{0}$$

From the expressions of the potential and kinetic energies, the equations of motion can be derived following an augmented Lagrangian technique:

$$\begin{aligned} \mathbf{M}(\mathbf{q})\, \ddot{\mathbf{q}} &= \mathbf{g}(\mathbf{q}, \dot{\mathbf{q}}, t) - \mathbf{\Phi}_{\mathbf{q}}^T \left(p\, \mathbf{\Phi} + k\, \boldsymbol{\lambda}\right) \\ \mathbf{0} &= k\, \mathbf{\Phi}(\mathbf{q}, t) \end{aligned}$$

$\mathbf{M}$ is the mass matrix, $\mathbf{\Phi}_{\mathbf{q}}$ is the constraint gradient, $\boldsymbol{\lambda}$ is the $m \times 1$ vector of Lagrange multipliers, the $n \times 1$ vector $\mathbf{g}$ represents the external, internal and complementary inertia forces, p and k are the penalty and scaling factors.

In a mechatronic system, additional equations are introduced for the various components of the control system, such as the actuators, the sensors and the controller. The dynamics of the control states could be represented by first-order ODEs, but, in order to allow a modular description using the block diagram language (Fig. 2), additional algebraic output variables $\mathbf{y}$ are required. The global interactions between the mechanical and control subsystems are represented by two vectors: the $n^{\mathbf{w}} \times 1$ vector $\mathbf{w}$ contains the sensor measurements exploited by the control system,

and it is associated with the displacements and velocities:

$$\mathbf{w} = \mathbf{L^{wq}}\mathbf{q} + \mathbf{L^{w\dot{q}}}\dot{\mathbf{q}}$$

where $\mathbf{L^{wq}}$ and $\mathbf{L^{w\dot{q}}}$ are sensor localization matrices. The $n^{\mathbf{a}} \times 1$ vector $\mathbf{g^a}$ represents the generalized forces exerted by the actuators on the mechanism. They contribute to a $n \times 1$ force vector $\mathbf{g}'$, which should be added to $\mathbf{g}$ in the mechanical equation:

$$\mathbf{g}' = \mathbf{L^{qa}}\mathbf{g^a}$$

where $\mathbf{L^{qa}}$ is the actuator localization matrix.

Referring to Fig. 2, each block or subsystem (k) is modelled by explicit state equations with respect to its inputs $\mathbf{u}^{(k)}$ and outputs $\mathbf{y}^{(k)}$:

$$\begin{aligned}\dot{\mathbf{x}}^{(k)} &= \mathbf{f}^{(k)}(\mathbf{u}^{(k)}, \mathbf{x}^{(k)}, t)\\ \mathbf{y}^{(k)} &= \mathbf{h}^{(k)}(\mathbf{u}^{(k)}, \mathbf{x}^{(k)}, t)\end{aligned}$$

Hence, one defines the global vectors of input, state and output variables, with respective dimensions v, s and t:

$$\mathbf{u} = \begin{bmatrix} \mathbf{u}^{(1)} \\ \vdots \\ \mathbf{u}^{(n^{block})} \end{bmatrix}, \qquad \mathbf{x} = \begin{bmatrix} \mathbf{x}^{(1)} \\ \vdots \\ \mathbf{x}^{(n^{block})} \end{bmatrix}, \qquad \mathbf{y} = \begin{bmatrix} \mathbf{y}^{(1)} \\ \vdots \\ \mathbf{y}^{(n^{block})} \end{bmatrix}$$

and the connectivity relations:

$$\mathbf{u} = \mathbf{L^{uw}}\mathbf{w} + \mathbf{L^{uy}}\mathbf{y}, \qquad \mathbf{g^a} = \mathbf{L^{ay}}\mathbf{y}$$

The coupled equations of motion are then derived:

$$\begin{aligned}\mathbf{M}(\mathbf{q})\ddot{\mathbf{q}} &= \mathbf{g}(\mathbf{q}, \dot{\mathbf{q}}, t) - \mathbf{\Phi}_{\mathbf{q}}^T(p\mathbf{\Phi} + k\boldsymbol{\lambda}) + \mathbf{L^{qy}}\mathbf{y}\\ \mathbf{0} &= k\,\mathbf{\Phi}(\mathbf{q}, t)\\ \dot{\mathbf{x}} &= \mathbf{f}(\mathbf{u}, \mathbf{x}, t)\\ \mathbf{0} &= \mathbf{y} - \mathbf{h}(\mathbf{u}, \mathbf{x}, t) - \mathbf{L^{y\ddot{q}}}\ddot{\mathbf{q}}\end{aligned} \tag{1}$$

where $\mathbf{L^{qy}} = \mathbf{L^{qa}}\mathbf{L^{ay}}$. The term $\mathbf{L^{y\ddot{q}}}\ddot{\mathbf{q}}$ has been added in the output equation in order to account for possible acceleration measurements. Indeed, one output variable y_j is introduced for each acceleration $\ddot{q}_i$ used in the control system, with the observer equation:

$$y_j = \ddot{q}_i$$

As a consequence, the acceleration variables still appear linearly in the coupled equations, which will be useful for the development of the integration algorithm.

The vector $\mathbf{u}$ does not contain any independent variable; it is simply a convenient notation for:

$$\mathbf{u} = \mathbf{L^{uq}}\mathbf{q} + \mathbf{L^{u\dot{q}}}\dot{\mathbf{q}} + \mathbf{L^{uy}}\mathbf{y}$$

with $\mathbf{L^{uq}} = \mathbf{L^{uw}}\mathbf{L^{wq}}$ and $\mathbf{L^{u\dot{q}}} = \mathbf{L^{uw}}\mathbf{L^{w\dot{q}}}$. Since $\mathbf{u}$ depends on $\mathbf{y}$, the algebraic variables $\mathbf{y}$ are implicitly defined by the output equation in (1), provided a regularity condition. Therefore, the control system has the structure of a semi-explicit index-1 DAE.

2.1 Transformation into second-order DAEs

In this section, the equations of motion are rewritten in a suitable form for the generalized-α algorithm. In order to transform the coupled equations into second-order DAEs, the auxiliary dynamic variables $\mathbf{z}$ and the vector $\mathbf{p}$ are defined:

$$\mathbf{z}(t) = \int_0^t \mathbf{x}(\tau)\, d\tau, \qquad \mathbf{p}^T = \left[\begin{array}{cc|cc} \mathbf{q}^T & \boldsymbol{\lambda}^T & \mathbf{z}^T & \mathbf{y}^T \end{array}\right]$$

$\mathbf{z}$ is only meaningful at the velocity level ($\dot{\mathbf{z}} = \mathbf{x}$) and at the acceleration level ($\ddot{\mathbf{z}} = \dot{\mathbf{x}}$). We obtain:

$$\boxed{\widehat{\mathbf{M}}(\mathbf{p})\ \ddot{\mathbf{p}} = \widehat{\mathbf{g}}(\mathbf{p}, \dot{\mathbf{p}}, t)} \tag{2}$$

with the singular matrix $\widehat{\mathbf{M}}$ and the vector $\widehat{\mathbf{g}}$:

$$\widehat{\mathbf{M}} = \left[\begin{array}{cc|cc} \mathbf{M} & \mathbf{0} & \mathbf{0} & \mathbf{0} \\ \mathbf{0} & \mathbf{0} & \mathbf{0} & \mathbf{0} \\ \hline \mathbf{0} & \mathbf{0} & \mathbf{I} & \mathbf{0} \\ -\mathbf{L}^{\mathbf{y}\ddot{\mathbf{q}}} & \mathbf{0} & \mathbf{0} & \mathbf{0} \end{array}\right], \qquad \widehat{\mathbf{g}}(\mathbf{p}, \dot{\mathbf{p}}, t) = \left[\begin{array}{c} \mathbf{g} - \mathbf{\Phi}_{\mathbf{q}}^T (p\mathbf{\Phi} + k\boldsymbol{\lambda}) + \mathbf{L}^{\mathbf{qy}}\mathbf{y} \\ -k\ \mathbf{\Phi} \\ \hline \mathbf{f} \\ -\mathbf{y} + \mathbf{h} \end{array}\right]$$

Since a Newton-Raphson procedure is implemented at each time-step, the linearized equations are required around any approximation $\mathbf{p}^*$, $\dot{\mathbf{p}}^*$ and $\ddot{\mathbf{p}}^*$. Defining the corrections of the displacements, velocities and accelerations:

$$\Delta\mathbf{p} = \mathbf{p} - \mathbf{p}^*, \quad \Delta\dot{\mathbf{p}} = \dot{\mathbf{p}} - \dot{\mathbf{p}}^*, \quad \Delta\ddot{\mathbf{p}} = \ddot{\mathbf{p}} - \ddot{\mathbf{p}}^*$$

and the residual vector $\mathbf{r}^* = \widehat{\mathbf{M}}(\mathbf{p}^*)\ \ddot{\mathbf{p}}^* - \widehat{\mathbf{g}}(\mathbf{p}^*, \dot{\mathbf{p}}^*)$, the linearized equations are:

$$\widehat{\mathbf{M}}\ \Delta\ddot{\mathbf{p}} + \widehat{\mathbf{C}}_t\ \Delta\dot{\mathbf{p}} + \widehat{\mathbf{K}}_t\ \Delta\mathbf{p} = -\mathbf{r}^* + \mathcal{O}\left(\Delta^2\right)$$

with the tangent matrices:

$$\widehat{\mathbf{K}}_t = \frac{\partial \mathbf{r}^*}{\partial \mathbf{p}} = \left[\begin{array}{cc|cc} \mathbf{K}_t & k\,\mathbf{\Phi}_{\mathbf{q}}^T & \mathbf{0} & -\mathbf{L}^{\mathbf{qy}} \\ k\,\mathbf{\Phi}_{\mathbf{q}} & \mathbf{0} & \mathbf{0} & \mathbf{0} \\ \hline -\mathbf{f}_{\mathbf{u}}\,\mathbf{L}^{\mathbf{uq}} & \mathbf{0} & \mathbf{0} & -\mathbf{f}_{\mathbf{u}}\,\mathbf{L}^{\mathbf{uy}} \\ -\mathbf{h}_{\mathbf{u}}\,\mathbf{L}^{\mathbf{uq}} & \mathbf{0} & \mathbf{0} & \mathbf{I} - \mathbf{h}_{\mathbf{u}}\,\mathbf{L}^{\mathbf{uy}} \end{array}\right], \quad \widehat{\mathbf{C}}_t = \frac{\partial \mathbf{r}^*}{\partial \dot{\mathbf{p}}} = \left[\begin{array}{cc|cc} -\partial\mathbf{g}/\partial\dot{\mathbf{q}} & \mathbf{0} & \mathbf{0} & \mathbf{0} \\ \mathbf{0} & \mathbf{0} & \mathbf{0} & \mathbf{0} \\ \hline -\mathbf{f}_{\mathbf{u}}\,\mathbf{L}^{\mathbf{u}\dot{\mathbf{q}}} & \mathbf{0} & -\mathbf{f}_{\mathbf{x}} & \mathbf{0} \\ -\mathbf{h}_{\mathbf{u}}\,\mathbf{L}^{\mathbf{u}\dot{\mathbf{q}}} & \mathbf{0} & -\mathbf{h}_{\mathbf{x}} & \mathbf{0} \end{array}\right]$$

$\mathbf{K}_t$ is the mechanical tangent matrix [1]: $\mathbf{K}_t = -\frac{\partial \mathbf{g}}{\partial \mathbf{q}} + \frac{\partial(\mathbf{M}\,\ddot{\mathbf{q}})}{\partial \mathbf{q}} + \frac{\partial\left(\mathbf{\Phi}_{\mathbf{q}}^T\,(p\,\mathbf{\Phi} + k\,\boldsymbol{\lambda})\right)}{\partial \mathbf{q}} \simeq -\frac{\partial \mathbf{g}}{\partial \mathbf{q}} + p\,\mathbf{\Phi}_{\mathbf{q}}^T\,\mathbf{\Phi}_{\mathbf{q}}$.

Those coupled equations are implemented in the Oofelie industrial finite element code [15]. The library of mechanical elements has been augmented by special elements for various generic blocks of the control system, e.g. a gain, an integrator or an ABCD linear time-invariant model. The vector $\widehat{\mathbf{g}}$ and the matrices $\widehat{\mathbf{M}}$, $\widehat{\mathbf{C}}$, $\widehat{\mathbf{K}}$ are implemented analytically at the element level, and constructed numerically according to the finite element assembly procedure at the system level.

3 Time integration algorithm

The generalized-α method relies on the Newmark implicit formulae, which are obtained from a Taylor series expansion of the displacements and velocities with respect to the time-step size h:

$$\begin{array}{l} \mathbf{p}_{i+1} = \mathbf{p}_i + h\ \dot{\mathbf{p}}_i + h^2\ (\frac{1}{2} - \beta)\ \mathbf{a}_i + h^2\ \beta\ \mathbf{a}_{i+1} \\ \dot{\mathbf{p}}_{i+1} = \dot{\mathbf{p}}_i + h\ (1 - \gamma)\ \mathbf{a}_i + h\ \gamma\ \mathbf{a}_{i+1} \end{array} \tag{3}$$

β and γ are constant numerical parameters. In the original Newmark scheme [2], the vector $\mathbf{a}$ is simply equal to the accelerations $\ddot{\mathbf{p}}$, whereas in the generalized-α method, it is defined by the linear recursion:

$$(1 - \alpha_m)\ \mathbf{a}_{i+1} + \alpha_m\ \mathbf{a}_i = (1 - \alpha_f)\ \ddot{\mathbf{p}}_{i+1} + \alpha_f\ \ddot{\mathbf{p}}_i, \quad \mathbf{a}_0 = \ddot{\mathbf{p}}_0 \tag{4}$$

where α_m and α_f are additional numerical parameters. In structural dynamics, the mass matrix is constant and a multiplication of this equation by $\widehat{\mathbf{M}}$ leads to the modified residual equation proposed by Chung and Hulbert [4]:

$$(1 - \alpha_m)\ \widehat{\mathbf{M}}\mathbf{a}_{i+1} + \alpha_m\ \widehat{\mathbf{M}}\mathbf{a}_i = (1 - \alpha_f)\ \widehat{\mathbf{g}}_{i+1} + \alpha_f\ \widehat{\mathbf{g}}_i, \quad \widehat{\mathbf{M}}\mathbf{a}_0 = \mathbf{g}_0 \tag{5}$$

The algorithm is self-starting and it can be implemented without explicit computation of the true acceleration $\ddot{\mathbf{p}}$. Indeed, equations (3) and (5) can be solved very efficiently for $\mathbf{q}$, $\dot{\mathbf{q}}$, and $\mathbf{a}$ according to a predictor-corrector procedure [16]. In many papers, equation (4) is not explicitly mentioned so that a confusion may appear between the acceleration-like variables $\mathbf{a}$ that come out of this algorithm and the true acceleration $\ddot{\mathbf{p}}$. In case of a non-constant mass matrix, the generalized-α method is still applicable, but equation (5) should not be exploited anymore. The scheme defined by equations (3) and (4) is equivalent to a two-step formula for the velocities and a three-step formula for the displacements [5].

For unconstrained mechanical systems, the second-order accuracy condition is:

$$\gamma = \frac{1}{2} + \alpha_f - \alpha_m$$

This condition clearly holds for unconstrained mechatronic systems, and a full convergence analysis is currently under study in the constrained case. The remaining free parameters β, α_f and α_m can be selected in order to obtain ideal numerical dissipation properties, as discussed in the following.

3.1 Spectral analysis

For linear first-order differential equations, the spectral properties of multistep methods are fully characterized by the generating polynomials, which are defined for a scalar test problem. Indeed, after the diagonalization of the equations, the numerical solution can be analysed independently for each scalar component. This diagonalization is also possible for undamped second-order ODEs, but not for a damped second-order system, since the mass, damping, and stiffness matrices cannot be simultaneously diagonalized. In a mechatronic system, the damping matrix accounts for the dynamics of the state variables and cannot be neglected; this makes the spectral analysis of the generalized-α method more complicated.

However, in the references [7, 17], close connections have been established between the global characteristic equation and two elementary characteristic polynomials: $P^{\mathbf{q}}_{h\omega}(\zeta)$ and $P^{\mathbf{x}}_{h\sigma}(\zeta)$. The former is defined for a scalar mechanical system $\ddot{q} + \omega^2\, q = 0$ and the second, for a scalar control system $\dot{x} = \sigma\, x$:

$$\begin{aligned} P^{\mathbf{q}}_{h\omega}(\zeta) &= (\zeta-1)^2\,[(1-\alpha_m)\zeta+\alpha_m] + (h\omega)^2[(1-\alpha_f)\zeta+\alpha_f][\gamma\zeta+1-\gamma+(\zeta-1)(\beta\zeta+1/2-\beta)] \\ P^{\mathbf{x}}_{h\sigma}(\zeta) &= (\zeta-1)\,[(1-\alpha_m)\zeta+\alpha_m] - h\sigma[(1-\alpha_f)\zeta+\alpha_f][\gamma\zeta+1-\gamma] \end{aligned}$$

Their asymptotic expressions are defined by:

$$P^{\mathbf{q}}_{\infty}(\zeta) = \lim_{h\omega\to\infty} \frac{P^{\mathbf{q}}_{h\omega}(\zeta)}{(h\omega)^2}, \qquad P^{\mathbf{x}}_{\infty}(\zeta) = \lim_{h\sigma\to\infty} \frac{P^{\mathbf{x}}_{h\sigma}(\zeta)}{h\sigma}$$

The results established in [7, 17] are summarized hereafter without formal proof.

The analysis relies on an elimination of the output variables, a diagonalization of the control state equations (the s complex eigenvalues are denoted σ_j) and a transformation of the mechanical equations into a canonical form. The mechanical coordinates $\mathbf{q}$ and $\boldsymbol{\lambda}$ are thereby decomposed into m constrained coordinates $\mathbf{q^c}$, m multiplier-like variables $\mathbf{q}^{\boldsymbol{\lambda}}$, and $\overline{n} = n - m$ independent modal coordinates $\mathbf{q^i}$ (the $\overline{n}$ eigenfrequencies are denoted ω_j). The contributions of the algebraic variables $\mathbf{y}$, $\boldsymbol{\lambda}$, and $\mathbf{q^c}$ turn out to be uncoupled in the characteristic equation, which has the following structure:

$$(P^{\mathbf{y}}(\zeta))^t\ \left(P^{\boldsymbol{\lambda}}(\zeta)\right)^m\ (P^{\mathbf{c}}(\zeta))^m\ P_{1\ldots\overline{n},1\ldots s}(\zeta) = 0$$

Each polynomial $P^{\mathbf{y}}$, $P^{\boldsymbol{\lambda}}$, and $P^{\mathbf{c}}$ is respectively associated with an output, a multiplier-like, or a constrained coordinate. Any root of those polynomials is also a root of $P^{\mathbf{q}}_{\infty}(\zeta)$, since we have:

$$P^{\mathbf{q}}_{\infty}(\zeta) = P^{\mathbf{c}}(\zeta) = P^{*}(\zeta)P^{\boldsymbol{\lambda}}(\zeta) = P^{*}(\zeta)P^{\mathbf{y}}(\zeta)$$

For uncoupled systems (e.g. $\mathbf{L^{qy}} = \mathbf{0}$), the characteristic polynomial associated with the dynamic variables $\mathbf{q^i}$ and $\mathbf{x}$ can be further factorized:

$$P_{1\ldots\overline{n},1\ldots s}(\zeta) = \prod_{j=1}^{\overline{n}} P^{\mathbf{q}}_{h\omega_j}(\zeta)\ \prod_{k=1}^{s} P^{\mathbf{x}}_{h\sigma_k}(\zeta)$$

Moreover, the coupling does not influence the numerical eigenvalues at high frequencies, since we have:

$$\begin{aligned} \lim_{\omega_j\to\infty} \frac{P_{1\ldots\overline{n},1\ldots s}(\zeta)}{(h\omega_j)^2} &= P^{\mathbf{q}}_{\infty}(\zeta)\ P_{1\ldots(j)\ldots\overline{n},1\ldots s}(\zeta) \\ \lim_{\sigma_j\to\infty} \frac{P_{1\ldots\overline{n},1\ldots s}(\zeta)}{h\sigma_j} &= P^{\mathbf{x}}_{\infty}(\zeta)\ P_{1\ldots\overline{n},1\ldots(j)\ldots s}(\zeta) \\ \lim_{h\to\infty} \frac{P_{1\ldots\overline{n},1\ldots s}(\zeta)}{h^{2\overline{n}+s}} &= (P^{\mathbf{q}}_{\infty}(\zeta))^{\overline{n}}\ (P^{\mathbf{x}}_{\infty}(\zeta))^s\ \kappa \end{aligned}$$

where $\mathcal{P}_{1\ldots(j)\ldots\overline{n},1\ldots s}$ (resp. $\mathcal{P}_{1\ldots\overline{n},1\ldots(j)\ldots s}$) is the characteristic polynomial after elimination of the contribution of q_j (resp. x_j), and κ is a constant depending on the parameters of the dynamic model.

In conclusion, for uncoupled mechatronic systems, the polynomials $P^{\mathbf{q}}_{h\omega}(\zeta)$ and $P^{\mathbf{x}}_{h\sigma}(\zeta)$ represent the full spectral behaviour of the numerical solution. For coupled problems, they still characterize the numerical dissipation in the high-frequency range, which is measured by the spectral radii at infinite frequency:

$$\rho^{\mathbf{q}}_{\infty} = \max\{|\zeta^{\mathbf{q}}_1|, |\zeta^{\mathbf{q}}_2|, |\zeta^{\mathbf{q}}_3|\}, \qquad \rho^{\mathbf{x}}_{\infty} = \max\{|\zeta^{\mathbf{x}}_1|, |\zeta^{\mathbf{x}}_2|\}$$

where $\zeta^{\mathbf{q}}_{1,2,3}$ are the roots of $P^{\mathbf{q}}_{\infty}(\zeta)$ and $\zeta^{\mathbf{x}}_{1,2}$ are the roots of $P^{\mathbf{x}}_{\infty}(\zeta)$. Both spectral radii should be in the interval $[0,1]$ for stability: a value of 1 means no dissipation, and a value of 0 means asymptotic annihilation of the high-frequency response.

3.2 Choice of the algorithmic parameters

The design of the algorithmic parameters of the generalized-α scheme has been addressed by Chung and Hulbert [4] and by Jansen et al [18]. Chung and Hulbert considered the simulation of lightly damped mechanical structures described by second-order ODEs. From an analysis of the roots of the polynomial $P^{\mathbf{q}}_{h\omega}(\zeta)$, they proposed an unconditionally stable scheme, which achieves an optimal compromise between accuracy at low frequencies and high-frequency numerical dissipation. Given a desired value of $\rho^{\mathbf{q}}_{\infty} \in [0,1]$, the other parameters are defined by:

$$\beta = \frac{1}{4}\left(\gamma + \frac{1}{2}\right)^2, \qquad \alpha_m = \frac{2\,\rho^{\mathbf{q}}_{\infty} - 1}{\rho^{\mathbf{q}}_{\infty} + 1} \qquad \text{and} \qquad \alpha_f = \frac{\rho^{\mathbf{q}}_{\infty}}{\rho^{\mathbf{q}}_{\infty} + 1} \qquad \text{(CH-}\alpha\text{ scheme)} \tag{6}$$

Jansen et al. [18] used the generalized-α method for the simulation of first-order differential equations in fluid dynamics. Their scheme is basically equivalent to our method for the state variables. Given a user-specified value of $\rho^{\mathbf{x}}_{\infty} \in [0,1]$, low-frequency dissipation is then minimized for:

$$\alpha_m = \frac{1}{2}\left(\frac{3\,\rho^{\mathbf{x}}_{\infty} - 1}{\rho^{\mathbf{x}}_{\infty} + 1}\right) \qquad \text{and} \qquad \alpha_f = \frac{\rho^{\mathbf{x}}_{\infty}}{\rho^{\mathbf{x}}_{\infty} + 1} \qquad \text{(JWH-}\alpha\text{ scheme)} \tag{7}$$

It is not necessary to define β, since this parameter is not used for the integration of $\mathbf{x}$.

Since unconditional stability is still observed when the CH-α scheme (resp. the JWH-α scheme) is applied to the first-order test equation (resp. to the second-order test equation), either scheme can be considered for the simulation of mechatronic systems. Cardona and Géradin [6] have shown that a marginally stable algorithm may become weakly unstable when applied to constrained systems. Therefore, a small amount of numerical dissipation is always required for the simulation of multibody systems. For coupled mechatronic problems, the spectral analysis in section 3.1 has shown that the numerical damping is still able to stabilize the numerical solution in the high-frequency range, even though global unconditional stability is only rigorously guaranteed in the uncoupled case. The CH-α scheme (6) and the JWH-α scheme (7) are not equivalent, which means that the user has to decide whether the algorithmic parameters should be optimized with respect to the mechanical system or to the control system. In the following applications, the critical dynamics lies in the mechanical subproblem, so that the CH-α scheme is naturally selected.

The next section presents some numerical results for two realistic applications, which are described in details in [7].

4 Applications

4.1 Vehicle semi-active suspension

The first application is a car equipped with a semi-active suspension. This benchmark has been identified in the framework of the Belgian Inter-University Attraction Pole on Advanced Mechatronic Systems (AMS-IAP5/06)[1].

Using a semi-active actuator in parallel with a passive spring, a control action is obtained by varying the restriction in current controlled valves. The control law exploits information from accelerometers mounted on the four corners of the chassis (Fig. 3), and from linear displacement sensors measuring the extension of the four shock-absorbers.

[1] Website of the AMS-IAP5/06: http://www.mech.kuleuven.ac.be/pma/project/ams

Figure 3: Audi A6 - corner accelerometers.

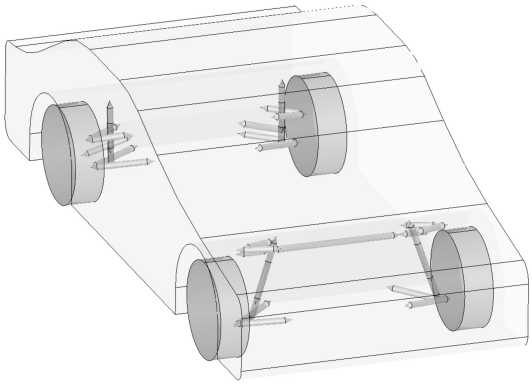

Figure 4: Mechanical model of the car.

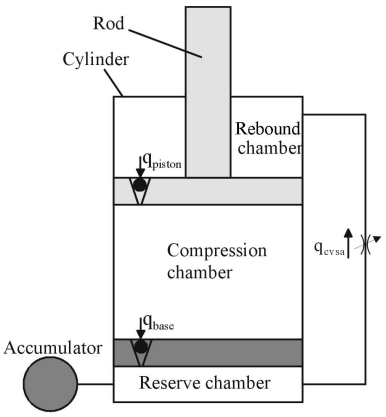

Figure 5: Semi-active damper.

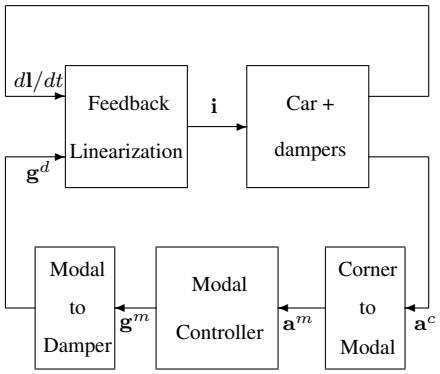

Figure 6: Semi-active control strategy.

The model of the mechatronic system is composed of a mechanical model, a model of the actuators, and a model of the controller. A detailed description of the actuators and of the controller is presented by Lauwerys et al. [19].

The rigid-body model of the car is illustrated in Fig. 4, and it includes the car-body, the suspension mechanisms, the slider-crank direction mechanism for the front wheels, and a model for the wheel/ground contact (lateral force, vertical force and yaw torque). The mechanical model involves about 600 degrees-of-freedom, and it could be later extended to include the stiffness of the suspension bushings, the flexibility of the chassis, and a longitudinal model for the wheels.

Fig. 5 illustrates the principle of a semi-active actuator. The actuator model is available in nonlinear state-space format:

$$\dot{\mathbf{x}}^{(damp)} = \mathbf{f}^{(damp)}(\mathbf{u}^{(damp)}, \mathbf{x}^{(damp)})$$
$$\mathbf{y}^{(damp)} = \mathbf{h}^{(damp)}(\mathbf{u}^{(damp)}, \mathbf{x}^{(damp)})$$

with the inputs, states and output:

$$\mathbf{u}^{(damp)} = [l \quad dl/dt \quad i]^T \qquad \mathbf{x}^{(damp)} = [p^{reb} \quad p^{comp}]^T \qquad \mathbf{y}^{(damp)} = [g^a]$$

l is the actuator extension, i, the electrical current in the valve, p^{reb} and p^{comp}, the pressures in the rebound and compression chambers, and g^a, the force exerted by the damper. The functions $\mathbf{f}^{(damp)}$ and $\mathbf{h}^{(damp)}$ are given by the manufacturer of the shock-absorber as C-functions.

The control law, available as a block diagram model, consists of three stages (Fig. 6): a feedback linearization (inverse actuator model), a transformation of the actuator forces and of the acceleration measurements into modal space (heave, roll, and pitch), and a linear integral control. In the figure, the vector $\mathbf{a}^c$ denotes the accelerations

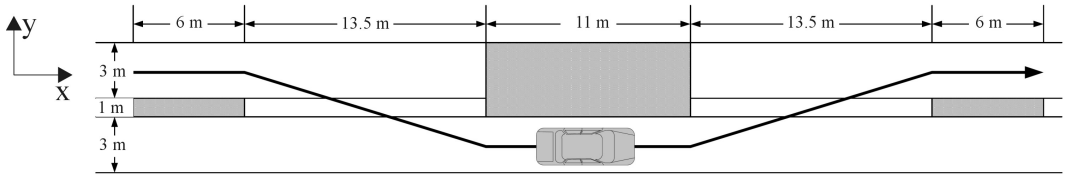

Figure 7: Lane change maneuver (standard qualification test).

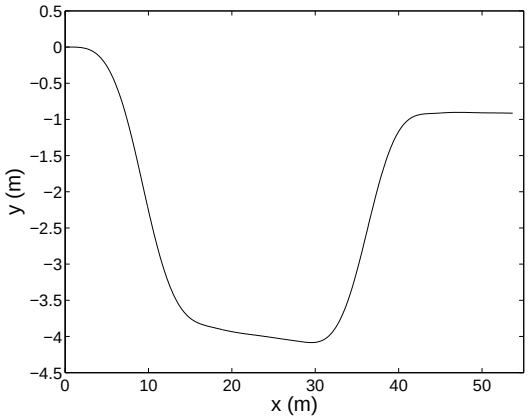

Figure 8: Horizontal trajectory of the car-body.

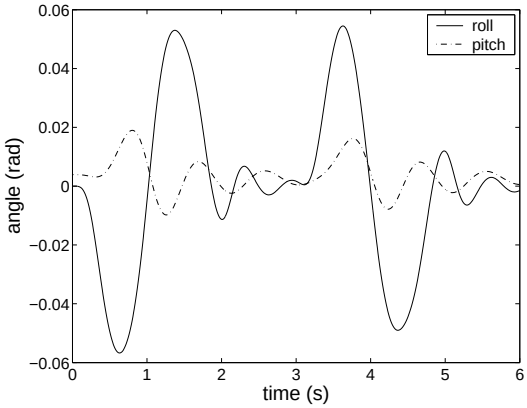

Figure 9: Angles of the car-body.

measured at the four corners of the car-body, $\mathbf{a}^m$, the modal accelerations, $\mathbf{g}^m$, the desired modal forces, $\mathbf{g}^d$, the desired damper forces, $d\mathbf{l}/dt$, the extension rates of the dampers, and $\mathbf{i}$, the electrical currents.

A lane change maneuver has been simulated (Fig. 7). The car has a 10 m/s initial velocity, and a driver applies an open-loop steering command, without any real-time correction (blind driver assumption). The motor and the brakes do not produce any torque on the wheels. The time-step of the simulation is 0.01 s and the algorithmic parameters are obtained for the CH-α scheme with $\rho_\infty^{\mathfrak{q}} = 0.9$. The simulation was carried out within a reasonable computational time (a few minutes on a desk computer).

Fig. 8 illustrates the horizontal trajectory of the car. Due to the lateral sliding of the wheels and the open-loop nature of the driving command, a lateral drift is observed in the trajectory. Fig. 9 presents the pitch and roll angles of the car-body. The dynamic behavior of the semi-active shock absorbers is analyzed in Fig. 10 and 11 (let us note that the model of the control system has been recently updated, which explains some differences in those results with respect to previous publications [7, 8]). Saturation phenomena dominate the variations of the electrical currents. The pressure in the compression chamber is very low in the extending phase, but it is close to the pressure in the rebound chamber in the compression phase. All those results are physically consistent, and can be of great use in a pre-prototyping design phase or to improve the control law.

4.2 Active control of a flexible manipulator

The second example concerns the motion and vibration control of an experimental robotic arm. The long-reach manipulator Ralf, shown in Fig. 12, has been developed at the Georgia Institute of Technology [20, 21]. It has a high payload to weight ratio, and it is stiff enough to achieve real-world applications. However, flexible effects in the links affect the positioning accuracy. Ralf has two kinematic degrees-of-freedom in a vertical plane, and it is actuated by two hydraulic cylinders. Two linear position sensing transducers, fixed to the hydraulic cylinder, measure the cylinder extension. Moreover, in order to detect the vibrations of the mechanism, two accelerometers are placed at the tip, in orthogonal directions.

As illustrated in Fig. 13, the control law is based on a composite two-time-scale strategy, which involves (i) a slow collocated controller, responsible for the trajectory tracking, (ii) a fast controller, which relies on both collocated measurements and tip acceleration measurements, in order to increase the damping in the flexible modes.

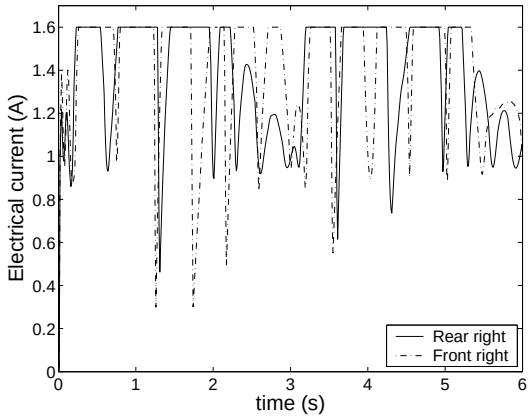

Figure 10: Electrical currents in the valves.

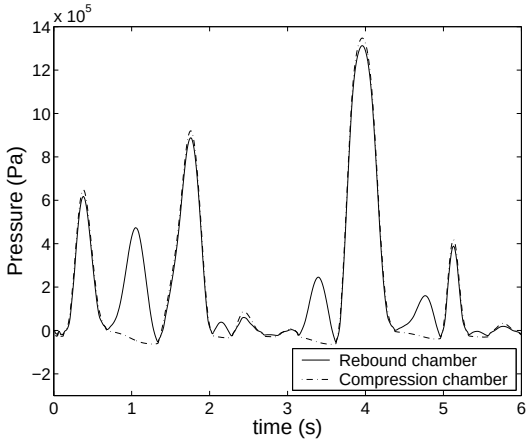

Figure 11: Hydraulic pressures in the rear right damper.

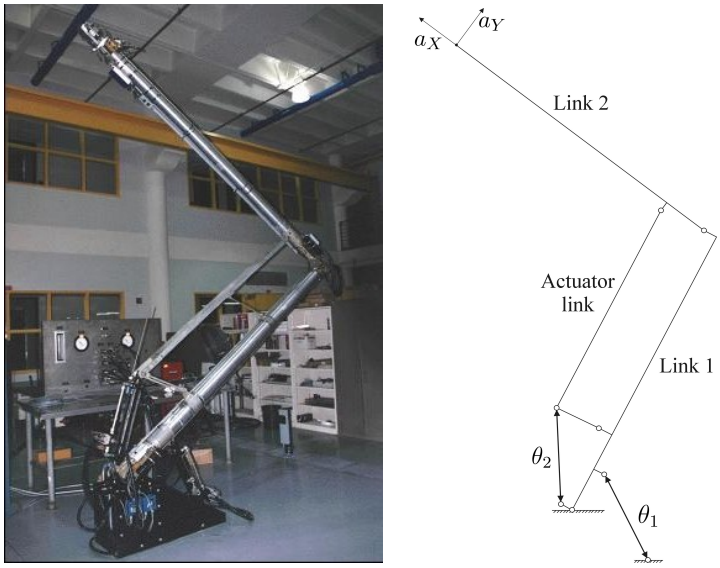

Figure 12: Ralf. θ_1 and θ_2 are the actuated degrees-of-freedom, whereas a_X and a_Y denote the measured accelerations.

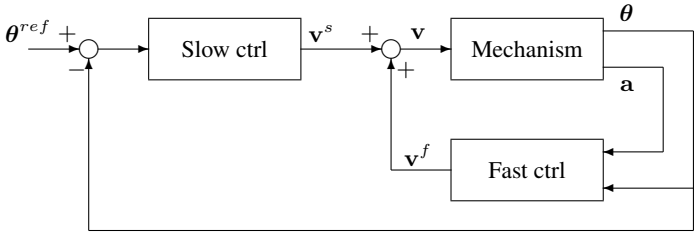

Figure 13: Two-time-scale control: $\mathbf{v}$ denotes the voltages applied to the hydraulic actuators.

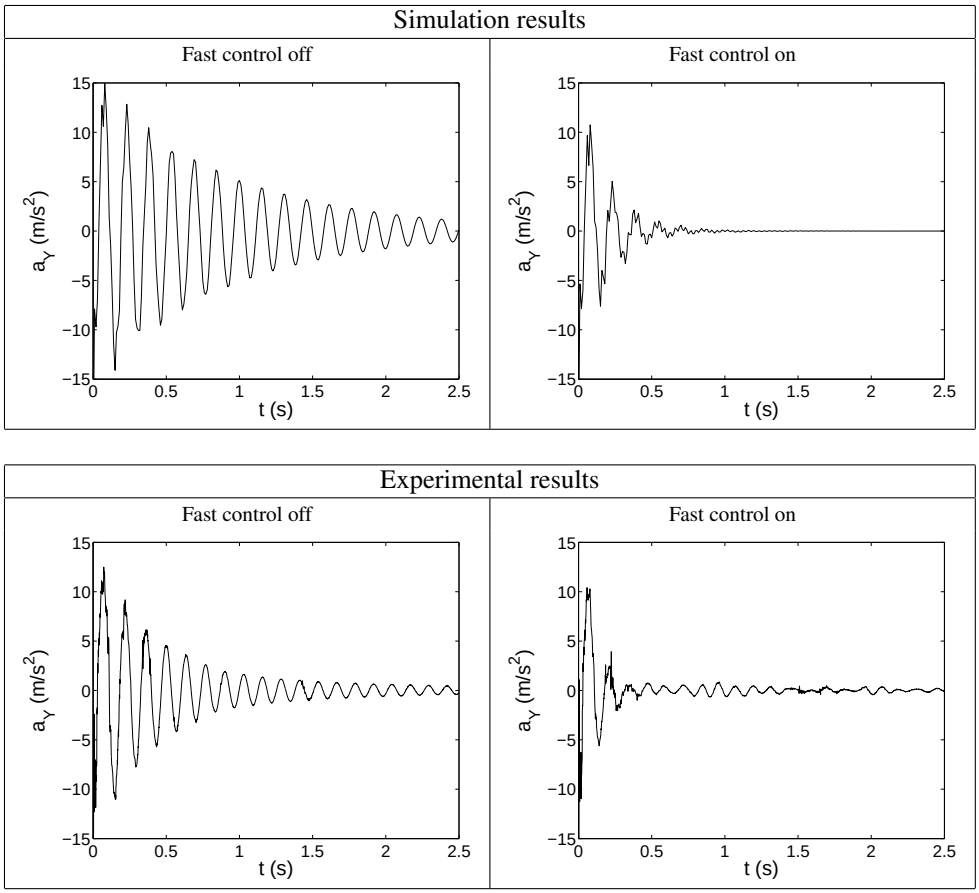

Figure 14: Tip response to a tip disturbance.

The model of the mechatronic system includes a model of the flexible mechanisms (link 1, link 2 and the actuator link are modeled as flexible beams), a linear dynamic model of the actuators obtained by experimental identification, and a block diagram model for the control law (equivalent to the model implemented in the real-time controller).

The step response to a tip vertical force is analyzed in Fig. 14. The time-step of the simulation is 0.01 s, and the algorithmic parameters are obtained for the CH-α scheme with $\rho_\infty^{\mathfrak{q}} = 0.7$. From these results, we conclude that the simulation tool predicts accurately the dynamic behaviour of the actual mechatronic system.

5 Conclusions

A generalized-α time-integration scheme has been presented for the dynamic analysis of mechatronic systems. The modelling formalism is based on the nonlinear finite element method and on the block diagram language, so that flexible mechanisms and control systems can be represented with a high degree of modularity.

The mechatronic system is described by a set of coupled first and second-order DAEs, which can be solved in the time domain following a strongly coupled strategy. In structural dynamics, the generalized-α time-integration method is second-order accurate, unconditionally stable, and it allows a controllable numerical dissipation at high-frequencies. For coupled mechatronic problems, the numerical dissipation properties are preserved, but global unconditional stability is only rigorously guaranteed for uncoupled problems. The algorithmic parameters can be optimized either with respect to the mechanical system (CH-α scheme) or to the control system (JWH-α scheme). A global convergence analysis is currently under study in the DAE case.

The implementation has been realized in the Oofelie industrial software, and two realistic applications have been

successfully analyzed: a car equipped with a complex semi-active suspension and a controlled flexible manipulator. For this last example, the simulation results are validated experimentally.

An extension of the simulation tool to account for sampled control systems is also reported in [7]. Future investigations will focus on the optimization of the computational efficiency using variable step-size methods and partitioned time-integration schemes. Indeed, one may select different algorithms (with possibly different step-sizes) for the mechanical system and the control system, in order to improve the compromise between accuracy and computational load.

Acknowledgement

M. Brüls is supported by a grant from the Belgian National Fund for Scientific Research (FNRS) which is gratefully acknowledged. This work also presents research results of the Belgian Program on Inter-University Poles of Attraction initiated by the Belgian state, Prime Minister's office, Science Policy Programming. The scientific responsibility rests with its authors. The authors thank Professor W.J. Book and his team from the Georgia Institute of Technology (Atlanta, U.S.) for making the Ralf setup available, and for contributing to the design and implementation of its vibration controller.

References

[1] M. Géradin and A. Cardona, Flexible Multibody Dynamics: A Finite Element Approach (John Wiley & Sons, New York, 2001).

[2] N. Newmark, A method of computation for structural dynamics, ASCE Jnl. Engrg. Mech. Div. **85**, 67–94 (1959).

[3] H. Hilber, T. Hughes, and R. Taylor, Improved numerical dissipation for time integration algorithms in structural dynamics, Earthquake Engineering and Structural Dynamics **5**, 283–292 (1977).

[4] J. Chung and G.M. Hulbert, A time integration algorithm for structural dynamics with improved numerical dissipation: The generalized-α method, J. of Applied Mechanics **60**, 371–375 (1993).

[5] S. Erlicher, L. Bonaventura, and O.S. Bursi, The analysis of the generalized-α method for non-linear dynamic problems, Computational Mechanics **28**, 83–104 (2002).

[6] A. Cardona and M. Géradin, Time integration of the equations of motion in mechanism analysis, Computers and Structures **33**, 801–820 (1989).

[7] O. Brüls, Integrated Simulation and Reduced-Order Modeling of Controlled Flexible Multibody Systems, Ph.D. thesis, University of Liège, Belgium (2005).

[8] O. Brüls, P. Duysinx, and J.-C. Golinval, A unified finite element framework for the dynamic analysis of controlled flexible mechanisms, in: Proc. of the ECCOMAS Conf. on Advances in Computational Multibody Dynamics, Madrid, Spain (2005).

[9] P. Lötsted and L. Petzold, Numerical solution of differential equations with algebraic constraints I: Convergence results for backward differentiation formulas, Mathematics of Computation **46**, 491–516 (1986).

[10] K.E. Brenan and B.E. Engquist, Backward differentiation approximations of nonlinear differential/algebraic systems, Mathematics of Computation **51**, 659–676 (1988).

[11] K.E. Brenan, S.L. Campbell, and L.R. Petzold, Numerical Solution of Initial-Value Problems in Differential-Algebraic Equations, second ed. (SIAM, Philadelphia, 1996).

[12] E. Hairer and G. Wanner, Solving Ordinary Differential Equations II - Stiff and Differential-Algebraic Problems, second ed. (Springer-Verlag, 1996).

[13] B. Owren and H.H. Simonsen, Alternative integration methods for problems in structural dynamics, Comp. Meth. Appl. Mech. Eng. **122**, 1–10 (1995).

[14] D. Negrut, R. Rampalli, G. Ottarsson, and A. Sajdak, On the use of the HHT method in the context of index 3 differential algebraic equations of multi-body dynamics. in: Proc. of the ECCOMAS Conf. on Advances in Computational Multibody Dynamics, Madrid, Spain (2005).

[15] A. Cardona, I. Klapka, and M. Géradin, Design of a new finite element programming environment, Engineering Computations **11**, 365–381 (1994).

[16] M. Géradin and D. Rixen, Mechanical Vibrations: Theory and Application to Structural Dynamics, second ed. (John Wiley & Sons, New York, 1997).

[17] O. Brüls and J.-C. Golinval, On the numerical damping of time integrators for coupled mechatronic systems, submitted to Comp. Meth. Appl. Mech. Eng. (2006).

[18] K.E. Jansen, C.H. Whiting, and G.M. Hulbert, A generalized-a method for integrating the filtered navier-stokes equations with a stabilized finite element method, Computer Methods in Applied Mechanics and Engineering **190**, 305–319 (2000).

[19] C. Lauwerys, J. Swevers, and P. Sas, Model free design for a semi-active suspension of a passenger car, in: Proc. of ISMA 2004, Leuven, Belgium (2004).

[20] J.D. Huggins, Experimental verification of a model of a two-link flexible, lightweight manipulator, Master's thesis, Georgia Institute of Technology (1988).

[21] T.R. Wilson, The design and construction of flexible manipulators, Master's thesis, Georgia Institute of Technology (1986).